Large pre-equilibrium contribution in $\alpha + {}^{nat}$Ni interactions at ≈8–40 MeV

Abhishek Yadav, Pushpendra P. Singh,* Manoj K. Sharma, Devendra P. Singh, Unnati, B. P. Singh,† and R. Prasad
Department of Physics, Aligarh Muslim University, Aligarh (UP) 202002, India

M. M. Musthafa
Department of Physics, Calicut University, Kerala, India

(Received 5 April 2008; published 8 October 2008)

To investigate pre-equilibrium emission of light nuclear particle(s), an experiment has been performed using α beams at the Variable Energy Cyclotron Center (VECC), Kolkata, India. In the present work, excitation functions for ^{58}Ni(α, p)^{61}Cu, ^{58}Ni(α, pn)^{60}Cu, ^{60}Ni(α, $p2n$)^{61}Cu, ^{60}Ni(α, n)^{63}Zn, ^{60}Ni(α, $2n$)^{62}Zn, ^{61}Ni(α, $3n$)^{62}Zn, and ^{61}Ni(α, $2n$)^{63}Zn reactions have been measured by using the stacked foil activation technique followed by off-line γ-ray spectroscopy. Experimentally measured excitation functions have been compared with the prediction of the theoretical model code ALICE-91 with and/or without the inclusion of pre-equilibrium emission. Analysis of the data suggests that an admixture of both equilibrium and pre-equilibrium emission is needed to reproduce experimental data at energies ≈8–40 MeV and reveals significant contribution from pre-equilibrium emission. An attempt has also been made to estimate the pre-equilibrium contribution, which has been found to depend on projectile energy and on number of emitted particle(s).

DOI: 10.1103/PhysRevC.78.044606 PACS number(s): 25.55.−e, 25.60.Dz, 25.70.Gh

Pre-equilibrium (PE) emission in light-ion-induced (LI-induced) reactions has been a topic of considerable interest during the past decade or so from both theoretical and experimental aspects, owing to the strong competition between equilibrium and the pre-equilibrium emission of light nuclear particles [1–4]. In PE emission, energetic light nuclear particles (neutrons and protons) are emitted predominantly at the initial stages of the nuclear interactions. The emission of light nuclear particles in the PE emission process followed by nonstatistical γ rays are assumed to arise from the interaction of the projectile with the target nucleons at the early stage of reaction. However, at later stages, a fully equilibrated compound nucleus (CN) may be formed and this nucleus further decays by statistical evaporation of light nuclear particles and/or characteristic γ radiations. Recent experiments have established that, at moderate excitation energies, the equilibrium decay is influenced by the emission of light nuclear particles before the equilibration of the composite system. Some of the important experimental signatures of PE emission that have emerged from the literature are (i) the presence of a larger number of high-energy light nuclear particles in the exit channel as compared to the number emitted in equilibrium decay, (ii) a forward-peaked angular distribution of light nuclear particles, and (iii) slowly decreasing tails of the excitation functions (EFs) [5–8]. A better understanding of these aforementioned characteristics of PE emission may provide important information about the involved reaction mechanism. The measurement and analysis of the EFs can be used as an informative probe of the PE emission process. In fact, the features of the EFs at low, medium, and high energies may reveal the characteristics of the involved reaction mechanism. The low-energy portion of EFs is dominated by the equilibrium decay; however, as the projectile energy increases the PE emission process becomes important and a slowly decreasing tail in the EFs becomes apparent [9–12]. Thus, the cross sections for emission of a given number of nucleons in a reaction may be measurable at energies where pure evaporative processes are greatly favored. To explain the PE emission of the highly excited composite system, several dynamical models have been proposed, including the internuclear cascade model (INC) [13,14], the quasifree scattering model (QFS) [15], and the pre-equilibrium EXCITON model [16–19]. The EXCITON model is considered to provide the most suitable description, particularly for α-induced reactions, in which the excitons—the excited particle (p) and hole (h)—are assumed to be produced through the interaction between projectile nucleons and target nucleus. These models have been used to describe various experimental data; however, the behavior of LI-induced reactions associated with the energy regime, entrance channel, mass asymmetry, etc. is still not well understood. Further, the LI-induced reactions are also important in basic research for the fundamental understanding of reaction dynamics and to test the validity of various available statistical model codes. Moreover, a rich set of experimental data on equilibrium and PE emission for various projectile-target combinations may be applicable in applied research on nuclear energy generation and/or waste management [20]. The experimental data on different reaction processes may also be useful in the production of medically important radionuclides and in reactor technology as well, particularly in the recently proposed Accelerator Driven Subcritical-reactor System (ADSS) [21,22]. This has led to a renewed interest in the study of nuclear reactions. With the motivation to study the interplay of equilibrium and pre-equilibrium emission processes, the EFs for seven α-induced reactions on natural nickel (^{nat}Ni) isotopes have been measured by using the stacked foil activation technique followed by off-line γ-ray spectroscopy.

*pushpendrapsingh@gmail.com
†bpsinghamu@gmail.com

TABLE I. List of reactions, identified characteristic γ rays, half-lives, branching ratios, and their Q values.

Reaction	Residue	J^{π}	Half-life	γ-ray energies (keV)	Branching ratio	Q value (MeV)
^{58}Ni(α, p)	^{61}Cu	$3/2^{-}$	3.33 h	283.0, 656.0	12.5, 10.7	−3.1
^{58}Ni(α, pn)	^{60}Cu	2^{+}	23.7 min	826.3, 1332.5	21.9, 88.0	−14.8
^{60}Ni(α, $p2n$)	^{61}Cu	$3/2^{-}$	3.33 h	283.0, 656.0	12.5, 10.7	−23.5
^{60}Ni(α, n)	^{63}Zn	$3/2^{-}$	38.47 min	669.86, 926.27	8.4, 6.6	−7.9
^{60}Ni(α, $2n$)	^{62}Zn	0^{+}	9.186 h	548.4, 596.7	15.2, 25.7	−17.0
^{61}Ni(α, $3n$)	^{62}Zn	0^{+}	9.186 h	548.4, 596.7	15.2, 25.7	−24.8
^{61}Ni(α, $2n$)	^{63}Zn	$3/2^{-}$	38.47 min	669.86, 926.27	8.4, 6.6	−15.7

The experiment has been performed at the Variable Energy Cyclotron Center (VECC), Kolkata, India. The ^{nat}Ni samples (prepared by rolling) of thickness ≈3.32 mg/cm^2 (measured by the α-transmission method) were pasted onto Al holders. A collimated α beam of ≈40 MeV has been allowed to fall on a stack of eight targets (each backed by an Al degrader of thickness ≈6.75 mg/cm^2) for ≈12 h with a beam current ≈100 nA. The average beam energy on a given target foil and degrader was calculated by using the code SRIM based on stopping power and range calculations. Post-irradiation analysis has been performed by using a high resolution, large volume (100 c.c.), precalibrated HPGe detector coupled with a data-acquisition system. The activities induced in various samples were recorded, leading to the production probability measurement of individual evaporation residues. Various standard sources of known strength were used to determine the efficiency of the detector at various source-detector separations. The sample-detector separations were suitably adjusted to minimize the dead time to ⩽10%. The residues produced from different reaction channels were identified by their characteristic γ rays, Q values, and decay-curve analysis. Further details of the experimental arrangement, formulation used, and data reduction procedure are similar to those in Ref. [23].

In the present work, the EFs for ^{58}Ni(α, p)^{61}Cu, ^{58}Ni(α, pn)^{60}Cu, ^{60}Ni(α, $p2n$)^{61}Cu, ^{60}Ni(α, n)^{63}Zn, ^{60}Ni(α, $2n$)^{62}Zn, ^{61}Ni(α, $3n$)^{62}Zn, and ^{61}Ni(α, $2n$)^{63}Zn reactions have been measured by using the activation technique followed by off-line γ spectroscopy. The reaction products identified on the basis of decay-curve analysis and Q-value systematics are given in Table I. In Table II the experimentally deduced production cross sections of identified residues are given. The errors quoted in the production cross sections are expected and are caused by several factors: (i) The statistical errors in counting of standard sources may introduce error in detector efficiency, which was minimized by accumulating the large number of counts for considerably longer time (≈5000 s). The geometry-dependent efficiency of γ-ray counting at various source-detector separations has been deduced and fitted with a fourth-order polynomial function, where the uncertainty from the fitting is found to be ⩽3% for the energy range of interest. (ii) The solid-angle effect is also expected to introduce some uncertainty in efficiency. This may be because the irradiated samples were not point sources like the standard sources. The errors in efficiency on account of the solid-angle effect have been calculated as demonstrated by Gardner *et al.* [24] and are found to be ⩽2%. (iii) The inaccurate determination of foil thickness and the nonuniformity of the foil may give rise to an uncertainty in the total number of target nuclei in the sample. The errors expected in the number of nuclei on account of the nonuniform thickness of the sample may be deduced by measuring the thickness at different positions of the sample and are found to be ≈1%. (iv) Proper care was taken to keep the beam current constant; however, all the fluctuations were noted during the entire irradiation time and the beam flux was individually calculated for the duration of fluctuations. The error from the fluctuations in the beam current was found to be ≈3%. (v) During irradiation of the stack, the beam traverses the thickness of the material, thus reducing the initial beam intensity. It is estimated that the error from this decrease in beam intensity is ⩽2%, as suggested by Ernst *et al.* [25]. The overall errors in the present measurement

TABLE II. List of reactions with their cross section and error.

Energy (MeV)	Cross section (mb)						
	^{58}Ni(α, p)	^{58}Ni(α, pn)	^{60}Ni(α, $p2n$)	^{60}Ni(α, n)	^{60}Ni(α, $2n$)	^{61}Ni(α, $3n$)	^{61}Ni(α, $2n$)
9 ± 1	150 ± 17	–	–	–	–	–	–
14 ± 0.9	360 ± 38	–	–	–	–	–	–
17 ± 0.9	401 ± 60	–	–	–	–	–	–
23 ± 0.8	201 ± 32	–	–	–	–	–	–
25 ± 0.8	95 ± 15	148 ± 22	–	–	11 ± 1.4	–	–
29 ± 0.8	46 ± 5	270.1 ± 40	–	21 ± 3	25 ± 4	–	124 ± 18
36 ± 0.7	16 ± 2	251 ± 38	64 ± 13	4 ± 0.9	28 ± 4	2 ± 0.8	151 ± 27
40 ± 0.7	13 ± 2	111 ± 17	191 ± 33	1 ± 0.3	17 ± 2	10 ± 0.7	75 ± 11

are found to be $\leqslant 15\%$. However, the uncertainties in the branching ratio, decay constant, half-lives, etc., which are taken from the table of isotopes [26], have not been taken into account in the measured cross sections. The experimentally measured EFs are compared with the calculations performed with the theoretical model code ALICE-91 [27], which takes both equilibrium and PE decay processes into account, and are shown in Figs. 1 and 2. The code ALICE-91 is frequently used for the analysis of experimental data [23,28]. This may be because of the fact that the input parameters of this code are few and are rather well defined. Moreover, the theoretical analyses with ALICE-91, in general, are found to give reasonably good agreement with the experimental data. The CN calculations in this code are performed by using the Weisskopf-Ewing model [29], whereas the PE component is simulated by using the geometry-dependent hybrid model [27]. The Myers-Swiatecki/Lysekil mass formula [30] is used for calculating Q values and binding energies of all the nuclei in the evaporation chain. Calculations for PE emission in this

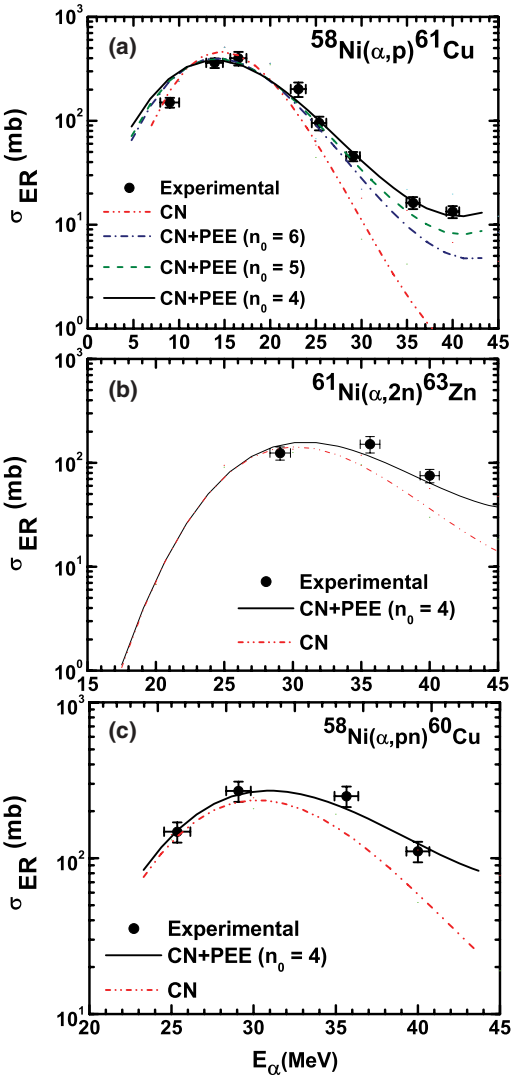

FIG. 1. (Color online) Experimentally measured and theoretically calculated EFs using the code ALICE-91.

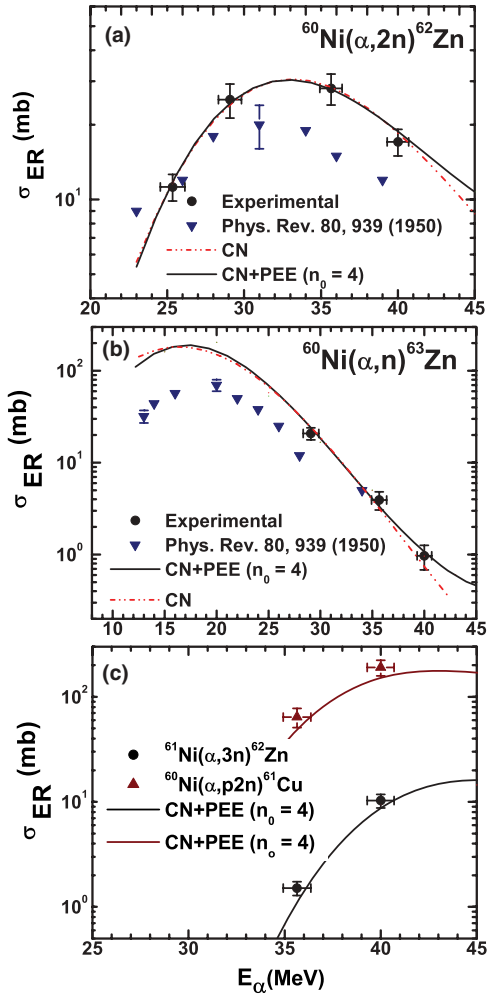

FIG. 2. (Color online) Experimentally measured and theoretically calculated EFs using code the ALICE-91.

code are done by assuming equipartition of energy among the initially excited particles and holes. The mean free path for intranuclear transition rates may be calculated either from the optical potential parameters of Becchetti and Greenlees [31] or from Pauli-corrected nucleon-nucleon cross sections [32,33].

In this code the level density parameter a, initial exciton number n_0, and the mean free path multiplier MFP are the important parameters that may be varied to reproduce the experimental data. The parameter a mainly affects the equilibrium component, whereas n_0 and MFP largely govern the pre-equilibrium component. In the hybrid model, the intermediate states of the system are characterized by the excitation energy E and number n_p of excited particles and number n_h of excited holes. Particles and holes are defined relative to the ground state of the nucleus and are called excitons. The initial configuration of the compound system defined by initial exciton number $n_0 = (n_p + n_h)$ is an important parameter of PE formalism. To find the value of the initial exciton number n_0, calculations for different values of n_0 were performed. As a representative case, calculated EFs for different values of n_0 ranging from 4 to 6 with configurations $n_0 = 4(2p +$

$2n + 0h$), $n_0 = 5(3p + 2n + 0h)$, and $n_0 = 6(3p + 2n + 1h)$ for the reaction ^{58}Ni(α, p)^{61}Cu are shown in Fig. 1(a). It may be pointed out that, in PE emission, the initial exciton number n_0 is a crucial quantity and determines the shape of the PE component. For α-induced reactions, values of initial exciton number $n_0 = 4$ or 5 have been justified by Blann [27] since a lower value of n_0 means a larger number of two-body interactions prior to the equilibration of the composite system, resulting in a large PE contribution. In the present work, a set of $a = A/8$, $n_0 = 4$, and $MFP = 1$ is found to satisfactorily reproduce the experimental data, in general. In the present work the same data set has been consistently used to obtain the cross-section values from the code. As shown in Figs. 1 and 2, the CN theoretical calculations satisfactorily reproduce the experimental data up to the peak portion of the EFs only. However, at higher energies (i.e., in the tail portion of the EFs) the admixture of CN and PE emission reproduce the experimental data to a satisfactory level.

Further, in some cases the same residual nucleus is produced through different reaction channels and hence the observed count rate may be the sum of contributions from different reaction paths. The residual nuclei ^{61}Cu, ^{62}Zn, and ^{63}Zn are found to be populated via equilibrium and/or pre-equilibrium decay of the CN formed through the interaction of ≈8–40 MeV α particles with various nickel isotopes. For example, the residual nucleus ^{61}Cu may be produced via both ^{58}Ni(α, p) and ^{60}Ni(α, $p2n$) reactions, where the Q values of these reactions are -3.1 and -23.5 MeV, respectively. Thus, for a projectile energy above 3.1 MeV, the production of ^{61}Cu will be entirely due to the ^{58}Ni(α, p) channel up to 23.5 MeV. However, at energies above 23.5 MeV the intensity of the γ rays from ^{61}Cu will make a contribution from both these reaction channels. From the measured cross section for ^{61}Cu above ≈24 MeV, the contribution of the theoretically calculated cross section was subtracted to obtain the contribution of ^{61}Cu populated via the ^{60}Ni(α, $p2n$)^{61}Cu reaction. The cross sections deduced for ^{60}Ni(α, $p2n$)^{61}Cu in this way are plotted in Fig. 2(c). As can be seen from this figure, the cross sections for the ^{60}Ni(α, $p2n$)^{61}Cu channel are very nicely reproduced by theoretical model predictions, which gives us confidence in the data-reduction procedure. Similarly, the cross section for ^{62,63}Zn populated via two different reaction channels as given in Table I have been obtained by using Q-value systematics. While deducing the cross section ratios proper care is taken for the threshold of each channel, isotopic abundance, half-life of the residual nucleus, and the branching ratio for the observed γ rays. Furthermore, the comparison of measured cross sections for the residues ^{62}Zn($2n$) and ^{63}Zn(n) has also been made with the pioneering measurements of Ghoshal [34] and are given in Figs. 2(a) and 2(b). As can be seen from Figs. 2(a) and 2(b), the data points of the present measurement are not in good agreement with the literature values [34]. In fact, the activities of ^{62}Zn and ^{63}Zn isotopes reported in Ref. [34] were deduced by a chemical separation method, which may involve quite large uncertainties because the activities were recorded by detecting energetic positrons with the help of a thin window counter. However, in the present work a much better high-resolution γ spectroscopy technique employing an HPGe detector has been used to provide a more reliable data set. Moreover, the trends of Ghoshal's data [34] are quite similar to the present measurements. It may further be pointed out that the present experimental data are very well fitted with the predictions of the code ALICE-91.

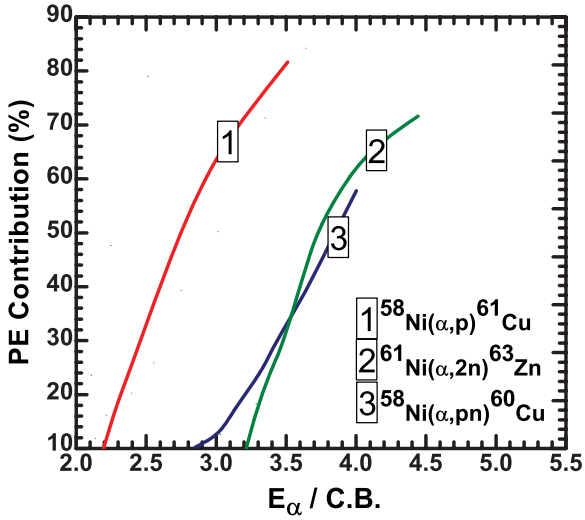

FIG. 3. (Color online) Estimated PE contribution as a function of normalized projectile energy (E_α/CB).

In the present work, the PE emission is significantly observed in some cases. Therefore, an attempt has been made to estimate the PE contribution at a given energy for a particular channel. It may be defined as the ratio of the pre-equilibrium cross section ($\sigma_{PE} = \sigma_{ER} - \sigma_{CN}$) to the evaporation residue cross section (σ_{ER}). The percentage PE contribution deduced from the analysis of data for different reaction channels has been plotted in Fig. 3 as a function of projectile energy normalized with the Coulomb barrier (E_α/CB). As can be observed from Fig. 3, in general, the percentage PE contribution is found to increase with normalized projectile energy. Furthermore, the threshold of PE emission for the different reaction channels is found to be different, depending on the associated Q value. It may, however, be pointed out that the PE contribution is found to be greater for the channels that consist of fewer PE particle(s)/nucleon(s) even at small projectile energy. This may be because the probability of single-nucleon emission is greater in the PE emission process. Moreover, it may not be out of place to mention that the PE contribution shows a dependence on initial excitation energy and/or Q value.

In summary, it may be inferred that the experimental data and the predictions of the statistical model code ALICE-91 reveal a significant contribution from the PE emission process at the studied energies. Furthermore, the input parameters—level density parameter $K = 8$, initial exciton number $n_0 = 4$ (with configuration $2p + 2n + 0h$), and $MFP = 1.0$—are found to be a suitable set of parameters to fit the experimental data in the present work. The percentage PE contribution for individual reaction products in different projectile-target combinations is found to be sensitive to the Q value of the reactions and/or the PE particle multiplicity. As such, it may be concluded that the PE emission is an important mode

of reaction in LI-induced reactions at the studied energies. Additional information about the PE emission may be obtained by PE particle(s) multiplicity and energy spectra measurement in equilibrium and PE emission processes, leading to the estimation of the entry point from PE emission to equilibrium processes.

The authors thank the Chairman, Department of Physics, and Director, VECC, Kolkata, India, for providing all the necessary facilities to carry out the experiment and analysis. A.Y. thanks the UGC, M.K.S. thanks the DST, and R.P. thanks the UGC and DST for providing financial support.

[1] N. Patronis *et al*., Phys. Rev. C **75**, 034607 (2007).
[2] T. E. Rodrigues, M. N. Martins, C. Garcia, J. D. T. Arruda-Neto, J. Mesa, K. Shtejer, and F. Garcia, Phys. Rev. C **75**, 014605 (2007).
[3] J. Pal *et al*., Phys. Rev. C **71**, 034605 (2005).
[4] W. Bauer and A. Botvina, Phys. Rev. C **52**, R1760 (1995).
[5] H. Feshbach, Rev. Mod. Phys. **46**, 1 (1974).
[6] H. Ejiri *et al*., Nucl. Phys. **A305**, 167 (1978).
[7] E. Gadioli, E. Gadioli-Erba, J. J. Hogan, and B. V. Jacak, Phys. Rev. C **29**, 76 (1984).
[8] J. Ernst *et al*., Z. Phys. A **328**, 333 (1987).
[9] M. Blann, Phys. Rev. Lett. **28**, 757 (1972); Phys. Rev. C **21**, 1770 (1980); M. Blann and H. Vonach, Phys. Rev. C **28**, 1475 (1983).
[10] H. Sakai, H. Ejiri, T. Shibata, Y. Nagai, and K. Okada, Phys. Rev. C **20**, 464 (1979).
[11] B. Strohmaier, M. Fassbender, and S. M. Qaim, Phys. Rev. C **56**, 2654 (1997).
[12] J. R. Wu and C. C. Chang, Phys. Rev. C **17**, 1540 (1978).
[13] M. L. Goldberger, Phys. Rev. **74**, 1269 (1948).
[14] K. Chen *et al*., Phys. Rev. C **4**, 2234 (1971).
[15] A. Mignerey, M. Blann, and W. Scobel, Nucl. Phys. **A273**, 125 (1976).
[16] J. J. Griffin, Phys. Rev. Lett. **17**, 478 (1966).
[17] M. Blann, Annu. Rev. Nucl. Sci. **25**, 123 (1975).
[18] D. Agassi, H. A. Weidenmüller, and G. Mantzouranis, Phys. Rep. **22**, 145 (1975).
[19] E. Gadioli, E. Gadioli-Erba, and P. G. Sona, Nucl. Phys. **A217**, 570 (1973).
[20] E. P. Gavathas, A. D. Frawley, R. C. Kline, and L. C. Dennis, Phys. Rev. C **51**, 1991 (1995).
[21] C. Rubbia *et al*., Report CERN/AT/95-94 (ET), 1995.
[22] B. P. Singh *et al*., Nucl. Instrum. Methods Phys. Res. A **562**, 717 (2006).
[23] M. K. Sharma *et al*., Eur. Phys. J. A **31**, 43 (2007), and references therein.
[24] R. P. Gardner *et al*., Nucl. Instrum. Methods **93**, 163 (1971).
[25] J. Ernst *et al*., Z. Phys. A **308**, 301 (1982).
[26] E. Browne and R. B. Firestone, *Table of Radioactive Isotopes* (Wiley, New York, 1986).
[27] M. Blann, NEA Data Bank, Report No. PSR-146, Gif-sur-Yvette, France (1991).
[28] M. K. Sharma *et al*., Phys. Rev. C **70**, 044606 (2004); Nucl. Phys. **A776**, 83 (2006).
[29] V. F. Weisskopf and D. H. Ewing, Phys. Rev. **57**, 472 (1940).
[30] M. L. Goldberger, Phys. Rev. **74**, 1269 (1948).
[31] F. D. Becchetti and G. W. Greenlees, Phys. Rev. **182**, 1190 (1969).
[32] K. Kikuchi and M. Kawai, *Nuclear Matter and Nuclear Reactions* (North-Holland, Amsterdam, 1968).
[33] M. Blann, Nucl. Phys. **A213**, 570 (1973).
[34] S. N. Ghoshal, Phys. Rev. **80**, 939 (1950).